A Comparison of Two Micromachined Inductors (Bar-Type and Meander-Type) For Fully Integrated Boost DC/DC Power Converters

Chong H. Ahn and Mark G. Allen
School of Electrical and Computer Engineering
Microelectronics Research Center
Georgia Institute of Technology
Atlanta, GA 30332-0250 U.S.A.

Abstract - **Two micromachined integrated inductors (bar-type and meander-type) are realized on a silicon wafer by using modified, IC-compatible, multilevel metallization techniques. Efforts are made to minimize both the coil resistance and the magnetic reluctance by using thick electroplated conductors, cores, and vias. In the bar-type inductor, a 25 μm thick nickel-iron permalloy magnetic core bar is wrapped with 30 μm thick multilevel copper conductor lines. For an inductor size of 4 mm x 1.0 mm x 110 μm thickness having 33 turns of multilevel coils, the achieved specific inductance is approximately 30 nH/mm² at 1 Mhz. In the meander-type inductor, the roles of conductor wire and magnetic core are switched, i.e., a magnetic core is wrapped around a conductor wire. This inductor size is 4 mm x 1.0 mm x 130 μm and consists of 30 turns of a 35 μm thick nickel-iron permalloy magnetic core around a 10 μm thick sputtered aluminum conductor lines. A specific inductance of 35 nH/mm² is achieved at a frequency of 1 Mhz. Using these two inductors, switched DC/DC boost converters are demonstrated in a hybrid fashion. The obtained maximum output voltage is approximately double an input voltage of 3 V at switching frequencies of 300 Khz and a duty cycle of 50% for both inductors, demonstrating the usefulness of these integrated planar inductors.**

I. INTRODUCTION

There is a large demand for the implementation of a fully integrated switched DC/DC converter on a chip or module. Applications for such converters include distributed power supplies for electronic systems or multichip modules as well as consumer products such as cellular telephones. An additional application area is integrated electrostatic microactuators [1], which usually require a drive voltage of several tens of volts or more, which is higher than commonly available integrated circuit power supply levels.

Inductive-based switched DC/DC converters are composed of switching control circuits and flyback inductive components. In realizing a DC/DC converter in an integrated fashion, integrated circuits for the switching function are already feasible; however, few planar integrated inductive components which have a sufficient quality factor (Q-factor) to act as a flyback inductor are available. Thus, the major obstacle in realizing an integrated switched DC/DC converter usually comes from the feasibility of planar integrated inductive components [2] with suitable electrical and magnetic characteristics.

In recent years, new micromachining techniques [1-3] have revolutionized the conventional concept of microstructure fabrication. These micromachining techniques provide several approaches for miniaturization of magnetic power components operated at high frequencies. Cores and conductors of several tens to hundreds of microns in thickness and width with good sidewalls and dimensional control can be easily fabricated. The higher electrical resistance of thin film magnetic cores and conductors helps reduce eddy current losses and skin depth losses. At the same time, conductor resistances on the order of several ohms or less is still achievable. In this study, by introducing an electroplated nickel/iron (Ni(81%)/Fe(19%)) permalloy [4] as a magnetic core, low temperature, CMOS-compatible fabrication is possible. The thin film nature of the core reduces eddy current losses; alternatively, the fabrication technique used is compatible with integrated laminations. Thus, hysteresis losses in cores which is a major concern in high frequencies may be controlled.

Prior to implementing a fully integrated DC/DC switched converter, a simple hybrid construction of a switched DC/DC converter using

0-7803-1456-5/94 $4.00 © 1994 IEEE

This work was supported in part by the National Science Foundation under Grant ECS-9117074.

the micromachined inductive components is fabricated to easily assess the feasibility of the integrated inductors. This hybrid prototype uses a bipolar transistor as the switching device and a diode as the complementary synchronized switch. The performance of the converters are compared in terms of the two inductors. Based on this information, fully integrated converters using the inductive components can then be designed.

II. FULLY INTEGRATED INDUCTORS

Since the fabrication technique of the micromachined inductors presented here is completely different from conventional methods used in the macro scale, feasible geometries in the micro scale are more limited. In addition, fabrication compatibility with integrated circuits is required to maximize the usefulness of the realized inductive components. The typical integrated circuit (IC) fabrication process constrains microstructures to be planar, with patterns made using various types of lithography. Consequently, the general geometries of microstructures feasible in the micro scale should be either 2-dimensional or quasi-3 dimensional.

In this work, two types of inductive components with closed magnetic circuits, the bar-type inductor and the meander-type inductor, are investigated. In particular, emphasis is placed on low temperature- CMOS-compatible fabrication, and high current carrying capacity of the fabricated inductive component.

A. Planar Integrated Bar-Type Inductor

In the conventional toroidal inductor, conductor wires wrapped around closed magnetic cores result in low leakage flux. Such structures (hereafter referred to as 'bar-type' inductors, since the core is in the form of a bar) have been fabricated using multilevel metal schemes to 'wrap' a wire around a magnetic core or air core. To demonstrate the feasibility of a planar toroidal inductor, such a component was fabricated by manually wrapping coils around a bar-type magnetic film core in [5]. It was verified from this structure that the introduction of a permalloy thin film increased the inductance value by a factor of 1000 when compared with an air core. However, this device was not fabricated in an integrated fashion.

In this work, microelectronic fabrication techniques are used to fabricate bar-type inductors with high current carrying capacity [2, 6]. The proposed inductor structure is depicted in Fig. 1. A feature of this inductor is that a closed (i.e. toroidal) magnetic circuit is achieved, minimizing the leakage flux and electromagnetic interference, and increasing the inductance value and the Q-factor. Thus, particular efforts have been made to minimize the coil resistance by increasing the thickness of the conductor lines and using electroplated vias.

Fabrication process starts with an oxidized (0.6 μm) 2-inch <100> silicon wafer as a substrate. A scanning electron micrograph of the fabricated structure is shown in Fig. 2, which was taken after dry-etching of the polyimide. In the bar-type inductor, a 25 μm thick nickel-iron permalloy magnetic core is wrapped with 30 μm thick multilevel copper conductor lines, constructing a conventional toroidal inductor in planar shape.

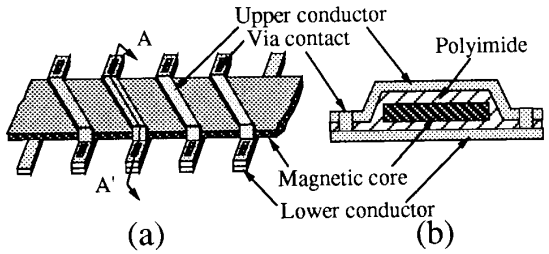

Fig. 1. Schematic diagram of the planar bar-type inductive component: (a) schematic view; (b) A-A' cut view.

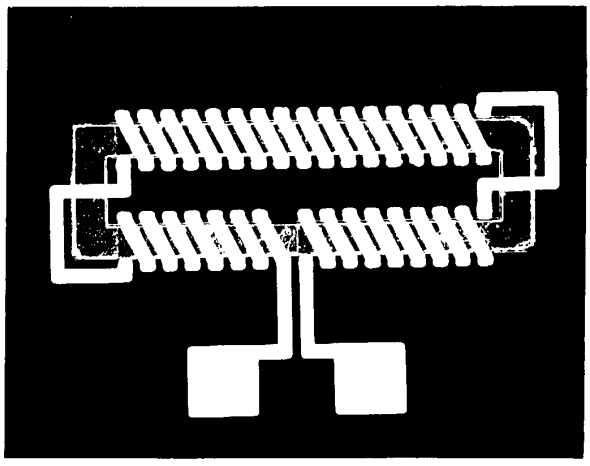

Fig. 2. Photomicrograph of the fabricated bar-type inductor.

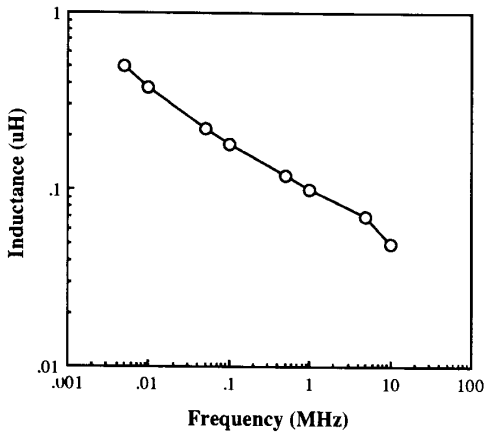

Fig. 3. Measured inductance of the fabricated bar-type inductor as a function of excitation frequency.

For an inductor size of 4 mm x 1.0 mm x 110 μm thickness having 33 turns of multilevel coils, the achieved inductance was approximately 30 nH/mm^2 at a frequency of approximately 1 MHz, corresponding to a core permeability of approximately 800. The width of conductor line and bar-core of this inductor are 80 *μm* and 300 *μm* respectively. The variation of the inductance with frequency is shown in Fig. 3. The measured dc resistance of the conductor line was approximately 0.3 ohms. The stray capacitance of the inductor was derived from the measured impedance and phase as a function of frequency using equivalent circuit analysis. From this analysis, the stray capacitance was shown to be in the several tens of *p*F region. The effect of the inductance falloff at higher frequencies shown in Fig. 3 is due to both the dependence of the permeability of the iron-nickel core on frequency and the effect of the stray capacitance. The maximum steady DC current which can be achieved in the bar-type is 2.5A, which gives a maximum allowable current density of 1x10^5 A/cm^2.

B. Planar Integrated Meander-Type Inductor

By interchanging the roles of the conductor and magnetic core in the bar-type inductor, i.e., by wrapping a magnetic core around a planar conductor, an analogous inductive structure can be achieved. A schematic drawing of a section of the integrated toroidal-meander type inductor [7-8], where toroidal refers to the core geometry and meander refers to the wrapping approach, is shown in Fig. 4. This meander geometry has an advantage over the bar-type geometry in that there are no electrical vias that add resistance to the conductor

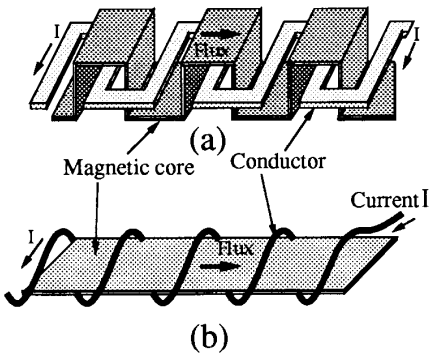

Fig. 4. Schematic diagrams of the integrated meander-type inductor and the more conventional toroidal type inductor. The structure of the two inductor schemes is analogous. (a) meander-type inductor; (b) toroidal-type inductor.

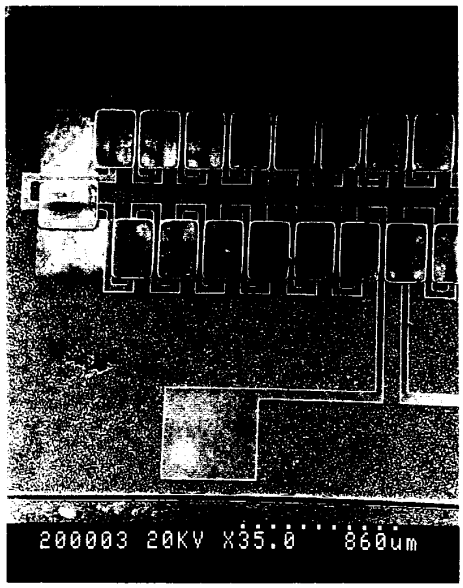

Fig. 5. Scanning electron micrographs of the fabricated meander-type inductor.

coil, since the conductor is located in a single plane. A disadvantage of the meander geometry is that the total length of magnetic core (and therefore the core reluctance) is approximately 5% longer than the core length of an analogous bar-type inductor.

The fabrication process also starts with oxidized (0.6 μm) 2-inch <100> silicon wafers as a substrate. Fig. 5 shows a scanning electron micrograph of the fabricated meander-type inductor. The total inductor size is 4 mm x 1.0 mm x 130 μm, i.e. the same inductor area as the bar-type; the coil has 30 turns; μ_r is 500; and the cross sectional areas of the magnetic core and the conductor coil are 300 μm x 35 μm and 50 μm x 8 μm respectively. The magnetic material used was electroplated Ni(81%)-Fe(19%) permalloy [4], and the conductor material used was sputter-deposited aluminum.

The measured inductance values as a function of frequency are plotted in Fig. 6. A fairly flat response through a frequency of 10 Mhz (approximately the limit of the impedance analyzer used) is observed. At a frequency of 1 Mhz, a specific inductance of 35 nH/mm^2 was achieved.

In this integrated inductor, the maximum current flowing through the conductor was measured as 2 A, which gives an attainable maximum current density of 5x10^5 A/cm^2. These values are 10^2-10^3 times larger than the values in the macro scale [9], which probably represents the large difference in surface-to-volume ratios of

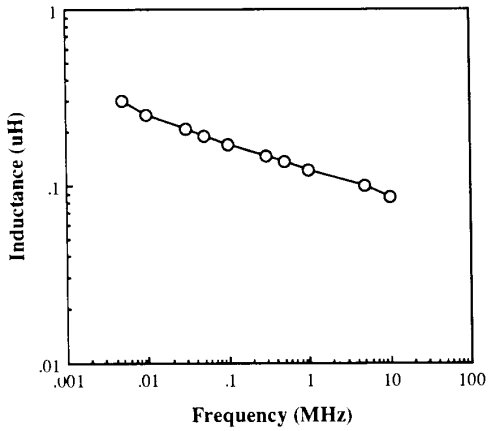

Fig. 6. Measured inductance of the meander-type inductor as a function of frequency.

conductors in the macro and micro scale, or the easy dissipation of the generated heat in the conductor because most of the meander conductors are exposed near the surface of the wafer.

The stray capacitance was shown to be in the *p*F region, and shown to have a negligibly small effect over the frequency ranges used. The effect of the inductance falloff at higher frequencies shown in Fig. 6 is due almost entirely to the dependence of the permeability of the iron-nickel core on frequency as described above.

III. SWITCHED DC/DC BOOST CONVERTERS

A prototype of a non-isolated, switched DC/DC boost converter [10] is shown in Fig. 7, which has a single transistor switch configuration. The duty ratio D is defined as the ratio of the switch-on time interval to the total switching interval T. In this converter, the output voltage is controlled by regulating the duty ratio of the switching bipolar transistor Q_1.

If the circuit shown in Fig. 7 is idealized by neglecting the internal resistances of the inductor, the transistor, and the diode, the theoretical voltage conversion gain is expressed as

$$\frac{V_0}{V_i} = \frac{1}{1-D} . \qquad (1)$$

In the designed DC/DC boost converter, an input voltage of 3 volts will be boosted up to 6 volts with D=0.5 at approximately 300 KHz. To choose the values of electrical parameters in the converter, it is assumed that the configurations of

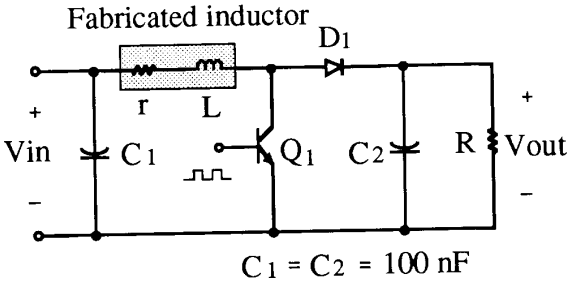

Fig. 7. Circuit diagram of the conventional switched DC/DC boost converter.

the designed converter are as follows: the output power is 40 mW (this power is comparable to the power required to operate an electrostatic microactuator), which requires a maximum output current of 6.7 mA.

However, the inductor, transistor, and diode shown in Fig. 7 actually include internal resistances denoted as r, r_{ts}, and r_d respectively, the theoretical voltage conversion gain expressed in Equation 1 is not appropriate in this case. Thus, the voltage conversion gain [11] can be written as

$$V_0 = \frac{V_i - (DV_{Q1} + D'V_D)}{D'} \frac{R}{R + (Dr_1 + D'r_2)/(D')^2} \quad (2)$$

where $r_1 = r + r_{ts}$, $r_2 = r + r_d$, $D' = 1 - D$, and V_{Q1} and V_D denote the voltage drops at the transistor Q_1 and the diode D_1 respectively.

The load resistance is varied from 5 ohms to 1.2 Mohms, and other electrical parameters are assumed as: $r = 1.2$ ohms; $r_{ts} = r_d = 0.5$ ohms; $V_{Q1} = 0.45$ V; and $V_D = 0.65$ V. As predicted and discussed in [11], an instability arises if the load resistance is less than 20 ohms, and then the dc output voltage jumps down to a lower level although the duty ratio increases. However, when the load resistance is much larger than the internal resistance, the output voltage is rapidly increased as the duty ratio increases, as shown to be in Fig. 9.

IV. DC/DC CONVERTER PERFORMANCE AND DISCUSSION

DC/DC boost converter circuits are then constructed in hybrid fashion using the fabricated inductive component as well as switching components described in Fig. 7.

The plot of output voltage variation for the various load resistances is shown in Fig. 8, where the switching frequency is 300 KHz, the duty cycle is 50 %, and the applied input voltage is 3 V. In both cases, the obtained output voltages for the various load resistance are increased and approach 6 V as the load resistance is increased.

The measured and the calculated output voltages as a function of duty cycle are plotted for both inductors in Fig. 9, with an input voltage of 3 V. The calculated output voltage is evaluated from Equation 2 using the electrical parameters

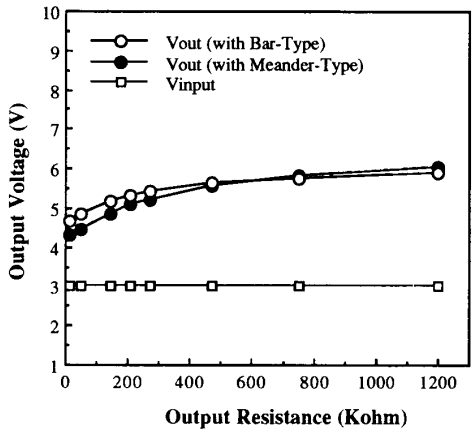

Fig. 8. Output voltage variation for the various load resistances, where the switching frequency is 300 KHz, the duty cycle is 50 %, and the input voltage is 3 V.

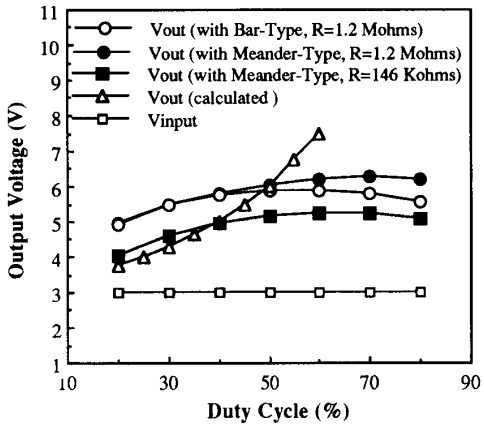

Fig. 9. Measured and calculated output voltages as the function of duty cycle at the input voltage of 3 V, where the calculated values are evaluated from the Equation 2 with the meander-type inductor.

measured from the meander-type inductor. The measured current flowing through the inductors is proportional to the duty cycle of the converter as shown in Fig. 10. This current reaches approximately 150 mA at a duty cycle of 50 % in the bar-type and the duty cycle of 70 % in the

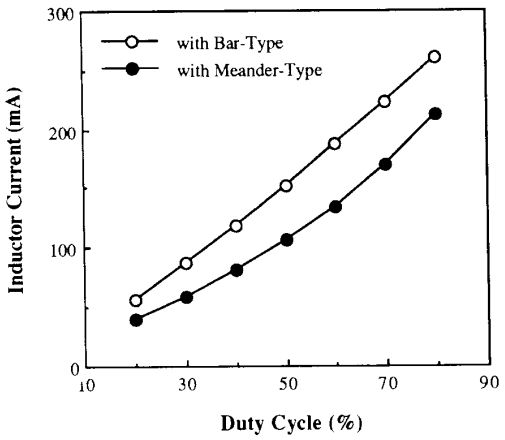

Fig. 10. Current flowing through the inductors as the function of duty cycle.

meander-type inductor. From the core geometries and the B-H characteristics of both inductors, inductor currents of 150 mA in the bar-type inductor and 180 mA in the meander-type inductor produce a flux density of 0.8 Tesla in the inductor cores. As reported in [3, 12], the permalloy core used in this study shows saturation above 0.8 Tesla. Thus, it is understandable from Fig. 9 that output voltages with the bar-type and the meander-type start to saturate above duty cycles of 50 % and 70 % respectively. Above a duty cycle of 50 %, the achievable output voltage with the meander-type inductor is higher than that with the bar-type inductor due to this magnetic flux saturation in the cores [12]. Since the output voltage can be continuously controlled as the duty cycle is adjusted, this integration feasible DC/DC boost converter has a high application potential for low voltage and micropower sources in an integrated fashion.

V. CONCLUSION

In this study, two planar integrated inductive components, a bar-type and a meander-type, are realized using micromachining and multilevel metal fabrication techniques. These components are suitable for magnetic micropower applications including miniaturized DC/DC converters. By using these two realized inductors, switched DC/DC boost converters are demonstrated in hybrid fashion.

In the bar-type inductor, an inductor size of 4 mm x 1.0 mm x 110 μm thickness having 33 turns of multilevel coils is realized, with an achieved specific inductance of approximately 30 nH/mm^2 at 1 Mhz. In the meander-type inductor, an inductor size of 4 mm x 1.0 mm x 130 μm thickness having 30 turns of multilevel cores is realized, with an achieved specific inductance of 35 nH/mm^2 at 1 Mhz. The fabrication sequence of these inductors is entirely compatible with post-processing of standard bipolar and CMOS circuitry, as well as the fabrication of multichip module substrates, thus enabling the integration of the inductor structure with control circuitry for applications such as filters, sensors, magnetic microactuators, and low-power voltage converters.

The inductors were evaluated in a prototype switched DC/DC boost converter. The obtained maximum output voltage is approximately double an input voltage of 3 V at a switching frequency of 300 Khz and a duty cycle of 50%, demonstrating the usefulness of these integrated planar inductors. The performances of DC/DC boost converters using both inductors are also compared. The feasibility of an integrated switched DC/DC converter using the micromachined inductive components has been demonstrated in this study. As the inductor realized in this research can potentially be integrated onto a chip or module, full DC/DC converter integration can be envisaged.

ACKNOWLEDGMENT

The authors would like to gratefully acknowledge DuPont and OCG Microelectronic Materials for their donations of polyimide and Lake Shore Cryotronics, Inc. for their assistance in measurements of the magnetic properties of the permalloy thin films. Technical discussions with Professor David Taylor of Georgia Tech are also gratefully acknowledged. Fabrication described in this paper was performed in the Microelectronics Research Center of the Georgia Institute of Technology.

REFERENCES

[1] L. S. Fan and Y.C. Tai and R. S. Muller, "IC-processed electrostatic micromotors", Sensors and Actuators, Vol. 20, pp. 41-47, 1989.

[2] C. H. Ahn, Y. J. Kim, and M. G. Allen, "A Fully Integrated Micromachined Toroidal

Inductor With a Nickel-Iron Magnetic Core (The switched DC/DC Boost Converter Application)", Transducers'93, Proc. 7th International Conference on Solid-State Sensors and Actuators, pp. 70-73, Yokohama, Japan, June 7-10, 1993.

[3] C. H. Ahn, "Micromachined components as integrated inductors and magnetic microactuators", Ph.D. Dissertation, Georgia Institute of Technology, Atlanta, GA, U.S.A, 1993.

[4] I. W. Wolf, "Electrodeposition of magnetic materials", Journal of Applied Physics, Vol. 33, No. 3, pp. 1152-1159, 1962.

[5] R. F. Soohoo, "Magnetic thin film inductor for integrated circuit application", IEEE Trans. Magn., vol. MAG-15, pp. 1803-1805, 1979.

[6] C. H. Ahn, Y. J. Kim, and M. G. Allen, "A Fully Integrated Planar Toroidal Inductor With A Micromachined Nickel-Iron Magnetic Bar", IEEE Transactions on Components, Hybrids, and Manufacturing Technology, 1993, in review.

[7] C. H. Ahn and M. G. Allen, "A new toroidal-meander type integrated inductor with a multilevel meander magnetic core", IEEE Trans. on Magnetics, MAG-30, No. 1, 1994.

[8] C. H. Ahn and M. G. Allen, "A fully integrated surface micromachined magnetic microactuator with a multilevel meander magnetic core", IEEE Journal of Microelectromechanical Systems, Vol. 2, No. 1, pp. 15-22, 1993.

[9] C. W. T. McLyman, Transformer and Inductor Design Handbook, New York, Marcel Dekker Inc., 1988, pp. 84-89.

[10] R. P. Severns and G. Bloom, Modern DC/DC Switchmode Power Converter Circuits, Van Nostran Reinhold Co., 1985, pp. 61-77.

[11] T. Ninomiya, K. Harada, and M. Nakahara, "On the maximum regulation range in boost and buck-boost converters", Proc. IEEE PESC, pp. 146-153, 1981.

[12] C. H. Ahn and M. G. Allen, "A planar micromachined spiral inductor for magnetic microactuator applications", Journal of Micromechanics and Microengineering, Vol. 3, No. 3, pp. 1-9, 1993.